

Mild Steel Corrosion Inhibition in a NaCl Solution by Lignin Extract of *Chromolaena odorata*

M.M. Muzakir,^{a,*} F.O. Nwosu^b and S.O. Amusat^b

^a Department of Chemistry, Gombe State University, P. M. B 127, Gombe, Nigeria

^b Department of Industrial Chemistry, University of Ilorin, P. M. B 1515, Ilorin, Nigeria

Received May 22, 2017; accepted June 2, 2018

Abstract

The inhibitive action of *Chromolaena odorata* stems extract, in various concentrations, against mild steel corrosion in a 1 M NaCl solution, was studied using weight loss, potentiodynamic polarization methods and scanning electron microscopy. Maximum inhibition efficiency of 99.83 % was obtained, at 303 K, for an extract concentration of 3000 mgL⁻¹. The activation and free energies for the inhibition reactions supported the physical adsorption mechanism. The extract adsorption onto the mild steel surface was found to be exothermic, spontaneous, and to obey the Langmuir adsorption model. FT-IR analysis showed the presence of hydroxyl (OH) and carbonyl(C=O) functional groups and aromatic rings in lignin, which are the binding groups that might be responsible for lignin's inhibitive action against mild steel corrosion. Furthermore, SEM analysis revealed that the mild steel surface was affected by lignin's adsorption, due to the formation of a protective film.

Keywords: lignin; potentiodynamic polarization; mild steel; adsorption; weight loss.

Introduction

Mild steel is one of the frequently used structural materials for storage tanks, reaction vessels, pipelines, and so on, in chemical and allied industries. During certain operations such as cleaning, pickling, de-scaling or even transportation, mild steel may come in contact with a sodium chloride solution, and get severely corroded [1]. In order to reduce the menace caused by the corrosion of industrial installations, several steps have been adopted. However, one of the best options available for protecting metals against corrosion involves the use of corrosion inhibitors. Corrosion inhibitors are widely used in industry to reduce the corrosion rate of metals and alloys in contact with aggressive environments [2]. These inhibitors can be adsorbed onto metal surfaces, block the active sites, and decrease the corrosion rate. The adsorption ability of inhibitors onto the metal surface depends on the metal's nature and surface charge, chemical composition

* Corresponding author. E-mail address: elmuzakir@gmail.com

of electrolytes, and on the molecular structure and electronic characteristics of the inhibitor's molecules [3].

Corrosion inhibitors' safety and environmental issues arisen in industries have always been a global concern. These inhibitors may cause reversible (temporary) or irreversible (permanent) damage to the kidneys or liver of terrestrial and aquatic organisms, or disturb their biochemical processes or enzyme systems [4]. Therefore, it is desirable to source for environmentally safe corrosion inhibitors. The exploration of natural products of plant origin as inexpensive and eco-friendly corrosion inhibitors is an essential field of study. In addition to being environmentally friendly and ecologically acceptable, plant products are biodegradable, low-cost, readily available and renewable sources of materials. Perhaps the most common natural substances used are plant extracts. Mild steel corrosion inhibition using different types of plant extracts has been investigated by many researchers [5-14].

Chromolaena odorata is an invasive deep-rooted shrub recorded as part of the 100 worst invasive species in the world [15]. It has widely spread throughout the tropics, and it has been declared as a noxious weed, due to the difficulty in controlling it by both curative and preventive measures [16]. Some researchers have reported the use of *C. odorata* leaves for mild steel and aluminum corrosion inhibition in HCl [17-20], H₂SO₄ acids [17] and also in artificial sea water [18]. It is important to also investigate mild steel corrosion in other solutions, such as NaCl, using other parts of *C. odorata* plant.

The aim of the present work is to investigate the corrosion inhibitive action of *C. odorata* stems extract on mild steel in a 1 M NaCl solution, using weight loss and potentiodynamic polarization methods.

Experimental

Material preparation

A mild steel sheet was commercially obtained, and its cut coupons had a percent composition (wt. %) of 98.79 % Fe, 0.15 % C, 0.63 % Mn, 0.07 % S and 0.36 % P. The sheet was 1.2 mm in thickness, and it was mechanically pressed cut into 3 × 2 cm coupons. These coupons were mechanically polished with emery papers of grade 200, 400 and 600. They were degreased in ethanol, dried in acetone and stored in moisture free desiccators, before their use in corrosion studies using weight loss methods.

Lignin extraction

A known amount of the powdered sample was weighed and placed in a round bottom flask, and a 5 M NaOH solution was charged into the flask, in the ratio of 1:10 (solid:liquid). The flask was equipped with a condenser, and heated at 100 °C, for 7 hours. The mixture was filtered to obtain a residue that was discarded, and its filtrate (black liquor) was precipitated with a 50 % H₂SO₄ solution. The precipitate (lignin) was washed several times with acidified water (pH 2). The lignin cake was first soaked dry under vacuum, and then dried in an oven at 50 °C, for 2 hours [19].

Solution preparation

A stock solution of 1 M NaCl was prepared using deionized water. This was used as solvent to prepare the lignin concentration by w/v ratio, in the range from 500 to 5000 mg/L.

Weight loss measurements

Experiments were performed at 30, 40, 50, 60, and 70 °C, with different concentrations (0.5 – 5 g/L) of the lignin extract. The immersion time for the weight loss measurements was 5 h. This was carried out using a Mettler Toledo XS64 electronic weighing balance, with the accuracy of ± 0.0001 g. All experiments were in triplicate, and illustrated data are mean values of the obtained results. From the weight loss average, the corrosion rate (CR), inhibition efficiency (IE) and surface coverage (θ), were calculated using equations 1, 2 and 3, respectively [20-21].

$$CR (mg\,cm^{-2}\,h^{-1}) = \frac{W}{At} \quad (1)$$

$$IE (\%) = \frac{W_1 - W_2}{W_1} \times 100 \quad (2)$$

$$\theta = \frac{W_1 - W_2}{W_1} \quad (3)$$

where W is the weight loss (mg), A is the exposed area (cm²) and t is the immersion time (h), whereas W₁ and W₂ are mild steel's weight, without and with inhibitor, respectively.

Potentiodynamic polarization studies

The electrochemical studies were performed using a VERSASTAT 400 complete dc voltammetry model and corrosion system, with V3 Studio software. The mild steel – cut into 1 cm², and exposed to the corrosive media with and without inhibitors – was used as working electrode, and Ag/AgCl rod as counter electrode. The reference electrode was a saturated calomel electrode (SCE), which was connected by a Luggin's capillary. The experiments were undertaken at 30 °C. The working electrode was immersed in a test solution for 1 h, until a stable open circuit potential was attained.

The Tafel analysis study was from cathodic potential of -250 mV to anodic potential of +250 mV, with respect to the corrosion potential, at a sweep rate of 1 mV/s. The linear Tafel segments of the anodic and cathodic curves were extrapolated to the corrosion potential, to obtain the corrosion current densities (i_{corr}). Each experiment was carried in triplicate to estimate reproducibility, and average values of the electrochemical parameters were reported. The inhibition efficiency was calculated using equation (4).

$$IE (\%) = \frac{i_{corr} - i_{corr(inh)}}{i_{corr}} \times 100 \quad (4)$$

where i_{corr} and $i_{corr(inh)}$ are the corrosion current densities obtained in uninhibited and inhibited solutions, respectively.

Surface analyses

Scanning Electron Microscope (FEI NOVA NANOSEM 230), which was equipped with an energy dispersive X-ray microanalysis (EDX) system (FEI, Eindhoven, Holland), was used to study the physical morphology and chemical analysis of the corroded mild steel surfaces. FT-IR spectroscopy (Shimadzu 8400 FTIR spectrometer) was used to collect the IR spectra of the dried lignin sample, as well as the mild steel corrosion product, in the presence of optimum lignin concentration.

Results and discussion

Effect of concentration and temperature

The corrosion rate and inhibition efficiency for mild steel in a 1 M NaCl solution at 303, 313, 323, 333 and 343 K, in the absence and presence of lignin extract, are given in Table 1. The corrosion rate is higher in the uninhibited solutions than in the inhibited solutions, which results from the mitigating effect of lignin on the mild steel corrosion rate. The corrosion rate decreased as the lignin extract concentration increased to 3000 mg/L. This suggests that, as the extract concentration increases, there is an increase in the number of extract constituents adsorbed onto the mild steel surface, which creates a barrier for mass transfer, and prevents further corrosion.

The inhibition efficiency progressively increases as the concentration of lignin increases up to 3000 mg/L, which is attributed to the increase in the fraction of the mild steel surface covered (θ) by lignin's adsorbed constituents, as its concentration increases. However, further increase in lignin concentration did not cause any increase in the inhibition efficiency; rather, the inhibition efficiency remained constant, or slightly decreased, in some cases. This might indicate that the inhibitor reaction onto the mild steel surface has reached the state of equilibrium. These results are similar to the findings reported in literature [22-23]. Maximum inhibition efficiency of 92.63 % was obtained at 30 °C (303 K), with 3000 mg/L of lignin extract.

It was also observed that mild steel CR, with and without lignin extract, increases with an increase in temperature. This is a result of the increase in the average kinetic energy of the reacting molecules. The inhibition efficiency (IE) decreased with an increase in temperature, which supports the mechanism of physical adsorption [20].

Effect of sodium chloride concentration

The effect of NaCl concentration on CR and IE was studied in the absence and presence of optimum lignin concentrations (3000 mg/L). The NaCl concentration was varied in the range from 0.5 to 2.5 M. The results are presented in Table 2. CR was observed to increase with an increase in NaCl concentration, in both uninhibited and inhibited solutions. This is because, as NaCl concentration

increases, the number of chloride ions in the solution which attack the steel surface also increases, which explains the increase in CR, as it was also reported in literature [24]. Consequently, the IE was found to decrease from 62.79 % to 53.33 %, as NaCl concentration increased from 0.5 to 2.5 M (Table 2). This can be attributed to the increase in the number of chloride ions at the steel surface, as the NaCl concentration increases, which hinders lignin molecules adsorption onto the steel surface, thereby decreasing the inhibition efficiency. Similar observation has been reported in literature [7].

Table 1. Corrosion parameters of mild steel in 1 M NaCl, in various concentrations of lignin extract, at different temperatures.

Temperature (K)	Inhibitor concentration (mgL ⁻¹)	CR (mg cm ⁻² h ⁻¹)	θ	IE (%)
303	Uninhibited	0.079	—	—
	500	0.055	0.6053	60.53
	1000	0.049	0.7789	77.89
	2000	0.043	0.8526	85.26
	3000	0.030	0.9263	92.63
	4000	0.031	0.9105	91.05
	5000	0.031	0.9005	90.05
313	Uninhibited	0.093	—	—
	500	0.065	0.5036	50.36
	1000	0.058	0.6750	67.50
	2000	0.051	0.7554	75.54
	3000	0.045	0.8179	81.79
	4000	0.037	0.8071	80.71
	5000	0.038	0.7893	78.93
323	Uninhibited	0.113	—	—
	500	0.077	0.4235	42.35
	1000	0.069	0.5897	58.97
	2000	0.060	0.6706	67.06
	3000	0.053	0.7294	72.94
	4000	0.046	0.7056	70.56
	5000	0.046	0.7001	70.01
333	Uninhibited	0.134	—	—
	500	0.091	0.3229	32.29
	1000	0.082	0.3913	39.13
	2000	0.071	0.4720	47.20
	3000	0.063	0.5279	52.79
	4000	0.054	0.5963	59.63
	5000	0.058	0.5652	56.52
343	Uninhibited	0.158	—	—
	500	0.108	0.3211	32.11
	1000	0.095	0.4	40.00
	2000	0.083	0.4737	47.37
	3000	0.075	0.5263	52.63
	4000	0.064	0.5947	59.47
	5000	0.069	0.5632	56.32

Immersion time effect

The results of the immersion time effect on CR and IE are shown in Table 3. CR and IE were calculated at 5 days interval for the total period of 30 days in NaCl,

without and with lignin optimum concentration (3000 mg/L), at 303 K. CR decreased as the immersion time increased to 20 days, and then slowly increased after 25 days of immersion. The continuous decrease in the corrosion rate could be attributed to the formation of an oxide film which shielded the mild steel surface from direct contact with the sodium chloride environment, and the later increase could be due to the destruction of the oxide film formed on the mild steel surface by the chloride ions [8].

Table 2. Corrosion parameters of mild steel in different concentrations of NaCl, without and with 3000 mg/L of lignin extract, at 303 K.

[NaCl]	Weight loss (mg)		CR (mg cm ⁻² h ⁻¹)		θ	IE (%)
	Uninhibited solution	Inhibited solution	Uninhibited solution	Inhibited solution		
0.5	8.6	3.2	0.143	0.053	0.6279	62.79
1.0	14.0	5.6	0.233	0.093	0.6000	60.00
1.5	19.3	8.0	0.322	0.133	0.5855	58.55
2.0	24.1	11.0	0.402	0.183	0.5436	54.36
2.5	30.0	14.0	0.500	0.233	0.5333	53.33

Table 3. Mild steel corrosion parameters in 1 M NaCl, without and with optimum lignin concentration (3000 mg/L), at different immersion times, at 303 K.

Immersion time (days)	Weight loss (mg)		CR (mg cm ⁻² h ⁻¹)		θ	IE (%)
	Uninhibited solution	Inhibited solution	Uninhibited solution	Inhibited solution		
5	54	37	0.038	0.026	0.3148	31.48
10	46	34	0.016	0.012	0.2609	26.09
15	38	29	0.009	0.007	0.2368	23.68
20	29	23	0.005	0.004	0.2069	20.69
25	65	46	0.009	0.006	0.2923	29.23
30	72	57	0.008	0.007	0.2083	20.83

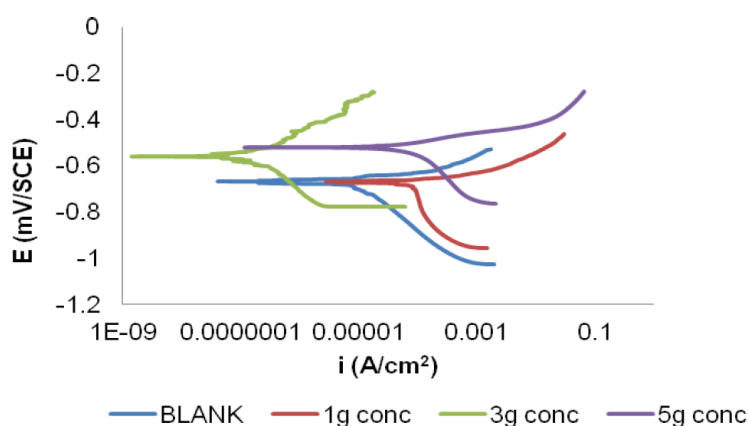


Figure 1. Anodic and cathodic polarization curves of mild steel in 1 M NaCl solutions, with and without different concentrations of lignin extract, at 30 °C.

The inhibition efficiency also decreased from 31.48 %, after 5 days of immersion, to 20.83 %, after 30 days of immersion time. Similar trend has also been reported by other researchers [9]. Generally, the extent of the decrease in

CR, IE % and surface coverage was slower for the inhibited solution than for the uninhibited solution.

Potentiodynamic polarization studies

Potentiodynamic polarization plots for mild steel corrosion in 1.0 M NaCl, with and without different concentrations of lignin extract, at 30 °C, are shown in Fig. 1.

The potentiodynamic polarization parameters obtained from these plots are given in Table 4, where it can be seen that the corrosion current density (i_{corr}) significantly decreased as the inhibitor concentration increased from 1000 to 3000 mg/L, with a corresponding increase in the inhibition efficiency (IE), reaching its maximum value of 99.83 % at 3000 mg/L.

Further increase in the inhibitor concentration caused a decrease in IE, which suggests that an optimum concentration has been reached. The inhibitor's presence caused a corrosion potential (E_{corr}) shift towards positive values, compared to that in the inhibitor's absence. The maximum displacement of E_{corr} in this work is lower than 85 mV. This indicates that the inhibitor is of the mixed type, suggesting that it affects both cathodic and anodic sites.

Table 4. Electrochemical parameters obtained from potentiodynamic polarization measurements of mild steel in 1.0 M NaCl, at various lignin concentrations.

Inhibitor concentration (mg/L)	$-E_{\text{corr}}$ (mV/SCE)	i_{corr} ($\mu\text{A}/\text{cm}^2$)	β_c (mV)	β_a (mV)	IE (%)
Uninhibited	674.38	796.10	3.80	2.17	-
1000	670.79	120.27	1.68	42.95	84.89
3000	557.11	1.32	847.68	1.02	99.83
5000	519.47	33.27	60.02	37.14	95.82

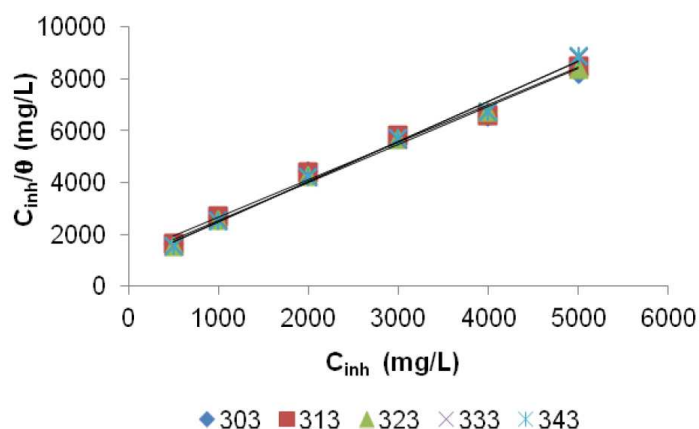


Figure 2. Langmuir adsorption isotherm plots for mild steel in 1 M NaCl, with different concentrations of lignin extract, at different temperatures.

Adsorption isotherms

The adsorption of inhibitor molecules onto the corroding metal surface has been considered as the root cause of corrosion inhibition. In order to consider lignin's adsorption process onto the mild steel surface, Langmuir adsorption isotherm was tested according to equation (5) [25].

$$\frac{C_{inh}}{\theta} = \frac{1}{K_{ads}} + C_{inh} \quad (5)$$

where θ is the surface coverage, K_{ads} is the equilibrium constant of the adsorption and C_{inh} is the inhibitor concentration.

Langmuir plots are shown in Fig. 2.

The experimental data were best described by Langmuir isotherm with the highest regression coefficient (R^2) close to 1, as shown in Table 5. The departure in the values of the slopes of Langmuir plots from unity may be due to the mutual repulsion or attraction between the adsorbed molecules in close vicinity, which may affect the heat of adsorption [1]. A modified Langmuir adsorption isotherm [26], given by the corrected equation, could be applied to this phenomenon.

$$\frac{C_{inh}}{\theta} = \frac{n}{K_{ads}} + nC_{inh} \quad (6)$$

The K_{ads} values were calculated from the intercept lines on the $\frac{C_{inh}}{\theta}$ axis that was plotted against C_{inh} . This is related to the standard free energy of adsorption (ΔG_{ads}), as reported elsewhere [21].

$$\Delta G_{ads} = -2.303RT \log(55.5 K_{ads}) \quad (7)$$

where 55.5 is the water concentration of the solution, in mL/L. ΔG_{ads} values for the inhibitor on the mild steel surface are also given in Table 5. ΔG_{ads} negative values indicate the stability of the adsorbed layer on the steel surface and the spontaneity of the adsorption process at all studied temperatures. ΔG_{ads} decreased (became more negative) with increasing temperatures, which indicated the occurrence of a favourable endothermic process [20]. More negative values reveal that inhibitors are strongly adsorbed onto the steel surface. Literature points that ΔG_{ads} values around -20 kJmol^{-1} or lower are related to the electrostatic interaction between the charged molecules and the charged metal (physisorption); those around -40 kJmol^{-1} or higher involve charge sharing or transfer from organic molecules to the metal surface, to form a coordinate type of bond (chemisorption) [27]. However, ΔG_{ads} obtained values lower than -30 kJmol^{-1} indicate that the lignin's adsorption mechanism tested on steel in a 1 M NaCl solution is physical adsorption.

Table 5. Langmuir isotherm parameters for lignin on mild steel in 1 M NaCl, obtained at different temperatures.

Temperature (K)	K_{ads} (mol^{-1})	n	R^2	ΔG_{ads} (kJ mol^{-1})
303	1241.5	1.399	0.9871	-28.07
313	1185.3	1.449	0.9879	-28.88
323	1051.4	1.473	0.9935	-29.48
333	937.03	1.546	0.9921	-30.07
343	905.96	1.558	0.9926	-30.88

Thermodynamic studies

Thermodynamic parameters, such as activation energy (E_a), enthalpy of adsorption (ΔH_{ads}) and entropy of adsorption (ΔS_{ads}) were determined, in order to get some insights into the possible energy effects of lignin adsorption onto the mild steel surface, in a 1 M NaCl solution.

Table 6. Activation parameters of mild steel dissolution in 1 M NaCl, without and with different lignin concentrations.

Inhibitor concentration (mg L ⁻¹)	E_a (kJmol ⁻¹)	R^2	ΔH^* (kJmol ⁻¹)	ΔS^* (Jmol ⁻¹ K ⁻¹)	R^2
Uninhibited	14.57	0.9992	11.98	-226.69	0.9991
500	14.02	1.0000	11.38	-231.64	0.9998
1000	13.89	0.9992	11.29	-232.88	0.9989
2000	13.69	0.9941	11.09	-234.63	0.9998
3000	14.12	0.9999	11.59	-234.08	0.9996
4000	15.19	0.9974	12.71	-232.02	0.9971
5000	16.82	0.9986	14.30	-226.81	0.9980

Determination of activation energy (E_a)

The activation energy (E_a) values were determined from Arrhenius plots for mild corrosion, by the following relation (equation 8):

$$\log CR = \log A - \frac{E_a}{2.303RT} \quad (8)$$

where A is the Arrhenius pre-exponential constant, T is the absolute temperature (K) and R is the universal gas constant (8.314 J/mol K). E_a values, as shown in Table 6, are lower in inhibited solutions than in uninhibited solutions, hence leading to a reduction in the corrosion rates, and suggesting that lignin molecules are strongly adsorbed onto the steel surface [28]. E_a values range (16.82–13.69 kJ/mol) is lower than the threshold value of 80 kJ mol⁻¹ required for chemical adsorption [17]. The Arrhenius plots are depicted in Fig. 3.

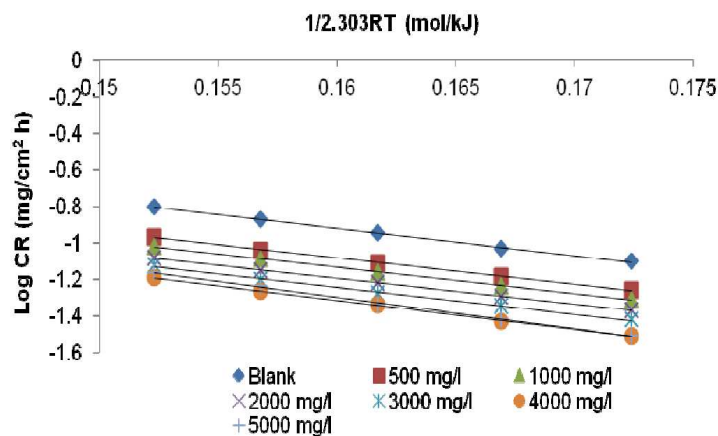


Figure 3. Arrhenius plots for mild steel in a 1 M NaCl solution, in the absence and presence of different lignin concentrations.

Determination of enthalpy and entropy of adsorption

Enthalpy (ΔH_{ads}) and entropy (ΔS_{ads}) of adsorption were estimated from transition state plots of $\log CR/T$ versus $1/T$, using equation (9).

$$\log\left(\frac{CR}{T}\right) = \left[\log\left(\frac{R}{hN}\right) + \left(\frac{\Delta S^*}{2.303R}\right)\right] - \frac{\Delta H^*}{2.303RT} \quad (9)$$

where h is the Planck's constant (6.6261×10^{-34} Js) and N is Avogadro's number (6.0225×10^{23} mol⁻¹). From the plot of $\log\left(\frac{CR}{T}\right)$ against $\frac{1}{T}$, enthalpy (ΔH^*) and entropy (ΔS^*) of activation were estimated from the slope and intercept, respectively. ΔH^* positive values reflect the endothermic nature of the steel dissolution process in the NaCl solution [29]. ΔH^* value decreases as lignin concentration increases up to 2000 mg/L, and thereafter it increases. The decrease in ΔH^* with increasing inhibitor concentrations reveals that the decrease in mild steel corrosion rates is not mainly controlled by kinetic parameters of adsorption [30]. The plots of $\log CR/T$ versus $1/T$ for mild steel corrosion in both uninhibited and inhibited 1 M NaCl solutions are depicted in Fig. 4. ΔH^* and ΔS^* values are shown in Table 6.

ΔS^* large and negative values, for mild steel dissolution in a 1 M NaCl solution, showed that the activated complex in the rate determining step represents an association rather than a dissociation step, meaning that a decrease in disordering took place on going from reactants to the activated complex. It is clear from the data listed in Table 6 that ΔS_{ads} values decreased more in the inhibited solution than in the uninhibited NaCl solution. In the uninhibited solution, the transition state of the rate determining recombination step represents a more orderly arrangement relatively to the initial state; so, a high value for the entropy of adsorption is obtained. In lignin's presence, however, the rate determining step is the reduction of dissolved oxygen, which forms water molecules. Since the surface is covered with lignin molecules, this will retard the reduction of dissolved oxygen at the metal surface, causing the system to pass from a random arrangement; hence, entropy of activation is decreased.

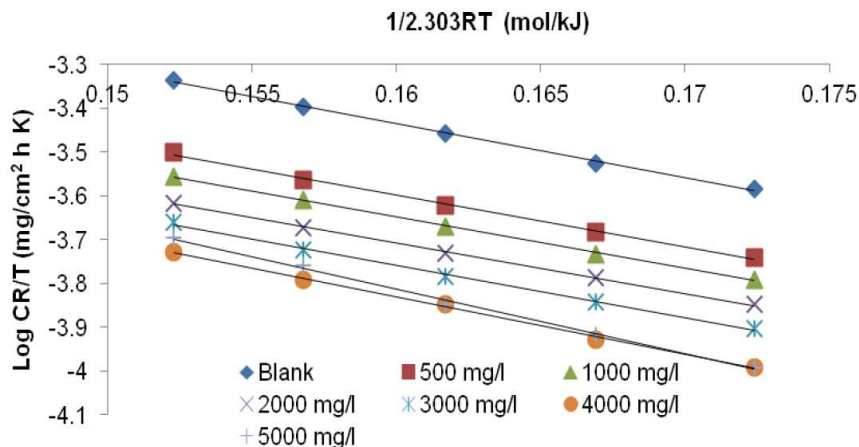


Figure 4. Transition state plots for mild steel in a 1 M NaCl solution, in the absence and presence of different lignin concentrations.

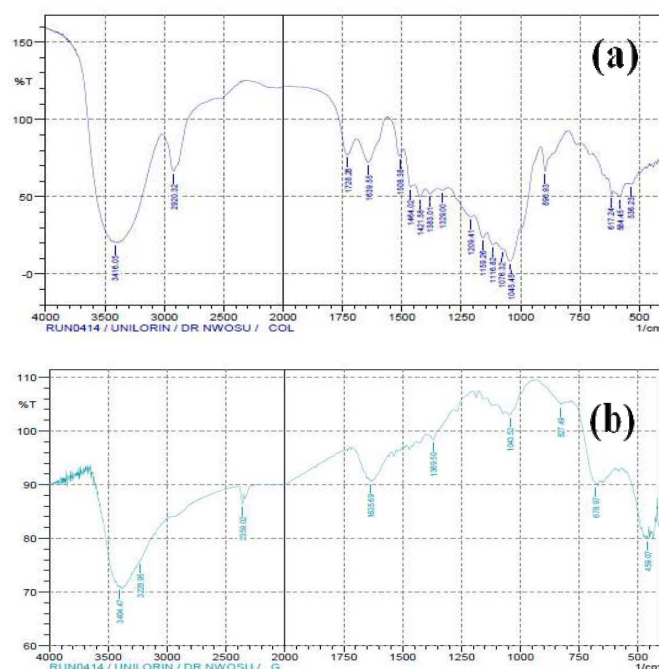


Figure 5. FT-IR spectra: (a) dried lignin extract; (b) film formed on the steel surface after 48 h of immersion in 1 M NaCl + 3000 mg/L of lignin extract at 30 °C.

FT-IR studies

The FT-IR spectra of lignin are shown in Fig. 5a, whereby the phenolic –OH stretching appeared at 3416 cm^{-1} . The peak at 2920 cm^{-1} can be assigned to aromatic C-H. The aromatic C=C stretching frequency appeared at 1639 cm^{-1} , while the value of 1728 cm^{-1} suggests C=O stretching frequency. The peaks at 1508 and 1421 cm^{-1} can be assigned to aromatic rings, due to aromatic skeletal vibrations. The peak at 1329 cm^{-1} is due to bending vibrations of OH groups, and the one at 1209 cm^{-1} is due to guaiacyl ring breathing with C-O stretching. The FT-IR spectrum of the protective film formed on the steel surface after immersion for a specific time in an inhibited solution is shown in Fig. 5b. Some of the peaks observed for lignin were also noticed for the protective film formed on mild steel immersed in 1 M NaCl containing 3000 mg/L of lignin extract. However, the phenolic –OH stretching has shifted from 3416 to 3404 cm^{-1} . The aromatic C-H stretching shifted from 2920 to 2359 cm^{-1} . The aromatic rings vibration has shifted from 1421 cm^{-1} to 1369 cm^{-1} . The bands at 827 and 459 cm^{-1} are probably originated mainly from α -FeOOH and γ -Fe₂O₃, respectively [20].

Surface morphology analysis

Scanning electron microscope (SEM) images show the physical surface morphology of mild steel in the absence and presence of the lignin inhibitor. SEM image (Fig. 6a) reveals that, in lignin's absence, the mild steel surface is damaged with pitted areas. This shape is typical of pitting corrosion [28]. The mild steel surface in lignin's presence (Fig. 6b), at the same magnification, shows a relatively smooth surface with deposited lignin extract. This is due to the

formation of an adsorbed protective film, or to the formation of ferric lignin as a barrier shield onto the exposed area.

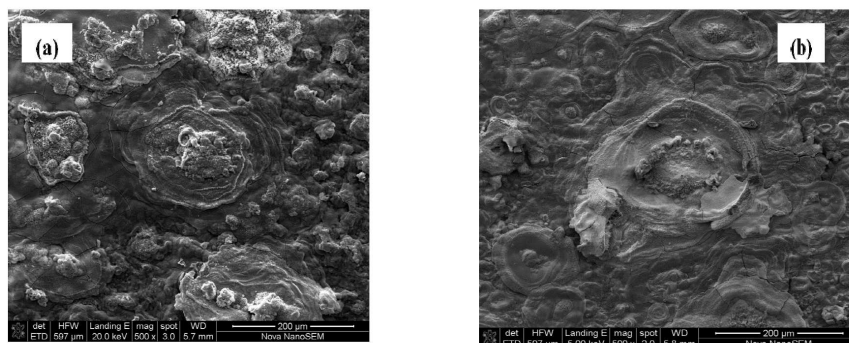


Figure 6. SEM micrographs for the mild steel surface specimens after 48 h of immersion in a 1 M NaCl solution: (a) without lignin extract; (b) with 3000 mg/L of lignin extract.

Mechanism of inhibition

Lignin's inhibitive action on mild steel corrosion in a NaCl solution can be attributed to the lignin molecules adsorption onto the mild steel surface via lone pairs of electrons on the oxygen atom of the lignin monomers. This is evident in the FTIR spectra of the corrosion products, in the inhibitor's presence, where there is a shift in frequency from 3416 cm^{-1} to 3404 cm^{-1} , for OH vibration, 2920 cm^{-1} to 2359 cm^{-1} for aromatic C-H stretching, and from 1421 cm^{-1} to 1369 cm^{-1} for the aromatic rings vibration (Table 7). There is also goethite ($\alpha\text{-FeOOH}$) vibration at 827 cm^{-1} .

Table 7. Summary of important peaks and shifts observed in the corrosion products.

Inhibitor wavenumber (cm^{-1})	Assignment	Corrosion products (in the inhibitor's presence) wavenumber (cm^{-1})
3416	phenolic OH group	3404
2920	aromatic C-H stretching	2359
1728	C=O stretching	-
1639	aromatic C=C stretching	-
1421	aromatic rings due to aromatic skeletal vibrations	1369
1329	bending vibrations of OH groups	-
1209	guaiacyl ring breathing with C-O stretching	-

Conclusions

Lignin extract of *Chromolaena odorata* was found to inhibit mild steel corrosion in a 1 M NaCl solution. The inhibition efficiency increased with increasing lignin concentrations, but decreased with an increase in temperature and sodium chloride concentrations. Maximum inhibition efficiency of 99.83 % was obtained with 3000 mg L^{-1} lignin concentration, at $30\text{ }^{\circ}\text{C}$. Adsorption energies were lower with inhibited solutions than in uninhibited solutions, suggesting a decrease in mild steel corrosion rate, while Gibb's free energy, enthalpy and entropy of adsorption indicate that the adsorption process was spontaneous and endothermic

in nature. The SEM and Langmuir adsorption isotherm studies suggested that the mechanism of corrosion inhibition occurred through an adsorption process.

References

1. Yadav M, Sharma U. Eco-friendly corrosion inhibitors for N80 steel in hydrochloric acid. *J Mater Environ Sci.* 2011;2:407-414.
2. Rajendran A, Karthikeyan C. The inhibitive effect of extract of flowers of cassia auriculata in 2 M HCl on the corrosion of aluminium and mild steel. *Int J Plant Res.* 2012;2:9-14.
3. Ismayil TI, Hany MA, Vagif MA, et al. Anti-corrosionability of some surfactants based on corn oil and monoethanolamine. *Am J Appl Chem.* 2013;1:79-86.
4. Singh A, Quraishi MA. Pipali (*Piper longum*) and Brahmi (*Bacopa monneiri*) extracts as green corrosion inhibitor for aluminium in NaOH solution. *J Chem Pharm Res.* 2012;4:322-325.
5. Kanchan A. Fenugreek leaves and lemon peel as green corrosion inhibitor for mild steel in 1 M HCl medium. *J Mater Sci Surf Eng.* 2014;1:44-48.
6. Sangeetha M, Rajendran S, Sathiyabama J, et al. Asafoetida extract (ASF) as green corrosion inhibitor for mild steel in sea water. *Int Res J Environ Sci.* 2012; 1:14-21.
7. Abd-El-Khalek DE, Abd-El-Nabey BA, Abdel-Gaber AM. Evaluation of nicotiana leaves extract as corrosion inhibitor for steel in acidic and neutral chloride solutions. *Port Electrochim Acta.* 2012;30:247-259.
8. Ibegbulam CM, Anyakwo CN, Ukoba OK, et al. Evaluations of inhibitive property of chromolaena odorata extract on aluminum in 1 M HCl and 0.5 M NaOH environment. *Pacific J Sci Technol.* 2011;12: 31-39.
9. Ikpeseni SC. Corrosion behaviour of mild steel in H₂SO₄ and NaCl solutions. *J Sci Multidiscip Res.* 2012;4:10-15.
10. Omotoyinbo JA, Oloruntoba DT, Olusegun SJ. Corrosion inhibition of pulverized jatropha curcas leaves on medium carbon steel in 0.5 M H₂SO₄ and NaCl environments. *Int J Sci Technol.* 2013;2:510-514.
11. Sharma SK, Mudhoo A, Jaina G, et al. Corrosion inhibition and adsorption properties of Azadirachta indica mature leaves extract as green inhibitor for mild steel in HNO₃. *Green Chem Lett Rev.* 2010;3:7-15.
12. Eddy NO, Odoemelam SA, Ama IN. Ethanol extract of Ocimum gratissimum as a green corrosion inhibitor for the corrosion of mild steel in H₂SO₄. *Green Chem Lett Rev.* 2010;3:165-172.
13. Eddy NO, Ita BI, Dodo SN, et al. Inhibitive and adsorption properties of ethanol extract of Hibiscus sabdariffa calyx for the corrosion of mild steel in 0.1 M HCl. *Green Chem Lett Rev.* 2012;5:43-53.
14. Beenakumari KS. Inhibitory effects of Murrayakoenigii (curry leaf) leaf extract on the corrosion of mild steel in 1 M HCl. *Green Chem Lett Rev.* 2011;4:117-120.
15. Ebrahim Akbarzadeh E, Ibrahim MNM, Rahim AA. Corrosion inhibition of mild steel in near neutral solution by kraft and soda lignins extracted from oil palm empty fruit bunch. *Int J Electrochem Sci.* 2011;6:5396-5416.

16. Tondoh JE, Kone AW, N'Dri JK, et al. Changes in soil quality after subsequent establishment of *Chromolaena odorata* fallows in humid savannahs. Ivory Coast. Catena. 2013;101:99-107.
17. Baxter J. *Chromolaena odorata*: weed for the killing or shrub for tilling. Agrofor Today. 1995;6-8.
18. Lora JH, Glasser WG. Recent industrial applications of lignin: A sustainable alternative to nonrenewable materials. J Polym Environ. 2002;10:39-48.
19. Khan MA, Ashraf SM. Development and characterization of groundnut shell lignin modified phenol formaldehyde wood adhesive. Ind J Chemical Technol. 2006;13:347-352.
20. Hamdy A, El-Gendy NS. Thermodynamic, adsorption and electrochemical studies for corrosion inhibition of carbon steel by henna extract in acid medium. Egypt J Petrol. 2013;2:1-9.
21. Olasehinde EF, Olusegun SJ, Adesina AS, et al. Inhibitory action of *Nicotiana tabacum* extracts on the corrosion of mild Steel in HCl: adsorption and thermodynamics study. Nat Sci. 2013;11:83-90.
22. Wabanne JT, Okafor V. Inhibition of the corrosion of mild steel in acidic medium by *Vernonia amygdalina*: adsorption and thermodynamics study. J Emerg Trends Eng Appl Sci. 2001;2:619-625.
23. Shyamala M, Kasthuri PK. The inhibitory action of the extracts of *Adathodavasica*, *eclipta alba*, and *Centellaasiatica* on the corrosion of mild steel in hydrochloric acid medium: a comparative study. Int J Corros. 2012;1-13.
24. Yunan P, Ibrahim K, Wan Nik WB. Effect of pH and chloride concentration on the corrosion of duplex stainless steel. Arab J Sci Eng. 2009;34:115-127.
25. Benali O, Benmehdi H, Hasnaoui O, et al. Green corrosion inhibitor: inhibitive action of tannin extract of *Chamaerops humilis* plant for the corrosion of mild steel in 0.5 M H₂SO₄. J Mater Environ Sci. 2013;4:127-138.
26. Hammouti B, Patel NS, Jauharian S, et al. Mild steel corrosion inhibition by various plant extracts in 0.5 M sulphuric acid. Int J Electrochem Sci. 2013;8:2635-2655.
27. Messali M, Asiri MAM. A green ultrasound-assisted access to some new 1-benzyl-3-(4phenoxybutyl) imidazolium-based ionic liquids derivatives – potential corrosion inhibitors of mild steel in acidic environment. J Mater Environ Sci. 2013;4:770-785.
28. Umoren SA, Obot IB, Obi-Egbedi NO. Corrosion inhibition and adsorption behaviour for aluminium by extract of *Aningeriarobusta* in HCl solution: synergistic effect of iodide ions. J Mater Environ Sci. 2011;2:60-71.
29. Ostovari AH, Peikari SM, Shadizadeh SR, et al. Corrosion inhibition of mild steel in 1 M HCl solution by henna and its constituents. Corros Sci. 2009; 51:1935-1947.
30. Bhat JI, Vijaya DPA. Meclizine hydrochloride as a potential non-toxic corrosion inhibitor for mild steel in hydrochloric acid medium. Arch Appl Sci Res. 2011; 3:343-356.